GEOPHYSICS, VOL. 72, NO. 5 (SEPTEMBER-OCTOBER 2007); P. E175–E183, 9 FIGS.
10.1190/1.2756600

Heavy oils: Their shear story

Jyoti Behura[1], Mike Batzle[2], Ronny Hofmann[3], and John Dorgan[4]

ABSTRACT

Heavy oils are important unconventional hydrocarbon resources with huge reserves and are usually exploited through thermal recovery processes. These thermal recovery processes can be monitored using seismic techniques. Shear-wave properties, in particular, are expected to be most sensitive to the changes in the heavy-oil reservoir because heavy oils change from being solid-like at low temperatures to fluid-like at higher temperatures. To understand their behavior, we measure the complex shear modulus (and thus also the attenuation) of a heavy-oil-saturated rock and the oil extracted from it within the seismic frequency band in the laboratory. The modulus and quality factor (Q) of the heavy-oil-saturated rock show a moderate dependence on frequency, but are strongly influenced by temperature. The shear-wave velocity dispersion in these rocks is significant at steam-flooding temperatures as the oil inside the reservoir loses viscosity. At room temperatures, the extracted heavy oil supports a shear wave, but with increasing temperature, its shear modulus decreases rapidly, which translates to a rapid drop in the shear modulus of the heavy-oil-saturated rock as well. At these low to intermediate temperatures (30°C–100°C), an attenuation peak corresponding to the viscous relaxation of the heavy oil is encountered (also resulting in significant shear-wave velocity dispersion, well described by the Cole-Cole model). Thus, shear-wave attenuation in heavy-oil rocks can be significantly large and is caused by both the melting and viscous relaxation of the heavy oil. At yet higher temperatures, the lighter components of the heavy oil are lost, making the oil stiffer and less attenuative. The dramatic changes in shear velocities and attenuation in heavy oils should be clearly visible in multicomponent seismic data, and suggest that these measurements can be qualitatively and quantitatively used in seismic monitoring of thermal recovery processes.

INTRODUCTION

High oil prices have focused new interest on heavy oil, considered as an unconventional hydrocarbon source. These energy resources have reserves that are estimated to be nearly triple the world reserves of conventional oil and gas (Curtis et al., 2002). Heavy oil is a type of crude oil that is highly viscous. The U. S. Department of Energy defines heavy oil as oil with API gravities between 10.0° and 22.3° (density at STP 1000 to 920 kg/m^3), although the exact relation between API gravity and viscosity is not straightforward.

The common characteristic properties are high specific gravity, low hydrogen-to-carbon ratio, high carbon residue, and high content of asphaltenes, heavy metals, sulfur, and nitrogen. It is believed that in most cases, the original crude oil was not heavy but a variety of biological (bacterial action), chemical, and physical processes degrade it into heavy oil (Hunt, 1996). Some of the largest known deposits are in the Athabasca sands in Canada, Faja del Orinoco in Venezuela, Alaska, California, Duri field in Indonesia, Russia, and China (Curtis et al., 2002).

The major challenge in exploiting heavy oil comes from its high viscosity, which makes production and transportation costly. Cold production of heavy oil from a reservoir usually has a recovery efficiency of less than 10%. Steam flooding, a common recovery process used by the industry, has a recovery efficiency as high as 80%. New technologies such as steam-assisted gravity drainage (SAGD) also have assisted in increasing the recovery.

Steam flooding and production change physical properties of the oil sand, such as velocity, density, and attenuation. These changes can potentially be inferred from time-lapse studies, thereby helping

Manuscript received by the Editor December 15, 2006; revised manuscript received May 1, 2007; published online August 2, 2007.
[1]Colorado School of Mines, Department of Geophysics, Center for Wave Phenomena, Golden, Colorado. E-mail: jbehura@mines.edu.
[2]Colorado School of Mines, Department of Geophysics, Center for Rock Abuse, Golden, Colorado. E-mail: mbatzle@mines.edu.
[3]Formerly Colorado School of Mines, Department of Geophysics, Center for Rock Abuse, Golden, Colorado; presently Shell International Exploration and Production Inc., Houston, Texas. E-mail: ronny.hofmann@shell.com.
[4]Colorado School of Mines, Department of Chemical Engineering, Golden, Colorado. E-mail: jdorgan@mines.edu.

in reservoir monitoring, as suggested by Nur et al. (1984). Recovery efficiency can be improved by monitoring the steam flood remotely using time-lapse seismic studies as done in the Duri field, Indonesia (Jenkins et al., 1997). Watson et al. (2001) uses traveltime-based methods to delineate areas of steam injection whereas Hedlin et al. (2001) find seismic-attenuation anomalies consistent with areas of steam injection. Schmitt (1999) observes significant differences between the sonic log velocities and VSP interval velocities within a heavy-oil-sand reservoir (Figure 1). Understanding such properties of these materials is essential to effective monitoring, because under some conditions the oil acts like a solid, whereas under other conditions, like a liquid. This is evident from Figure 2, where the heavy oil seems to be a solid at room pressure and temperature, but on heating melts and thus would attenuate shear waves.

Laboratory measurements are necessary to understand the physical changes that accompany heating of heavy-oil rocks. However, few laboratory studies have been carried out. Nur et al. (1984) study the influence of temperature on the velocities and attenuation of glycerol-filled Boise sandstones and on oil sands. Han et al. (2005) look at the shear-wave velocity in heavy oils. Batzle et al. (2005, 2006) also measure velocities and attenuation in heavy oils. Most of the above laboratory measurements are ultrasonic, and results do not necessarily apply in the seismic bandwidth.

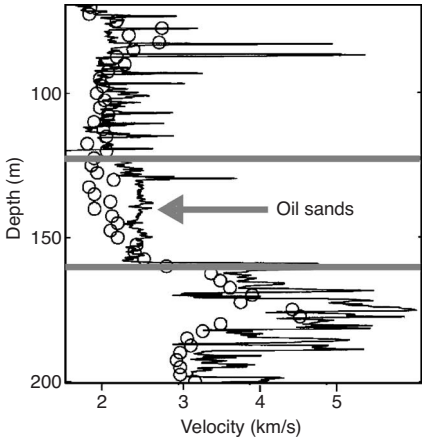

Figure 1. Sonic log velocities (line) and VSP interval velocities (open circles) in a well through oil sands (Schmitt, 1999).

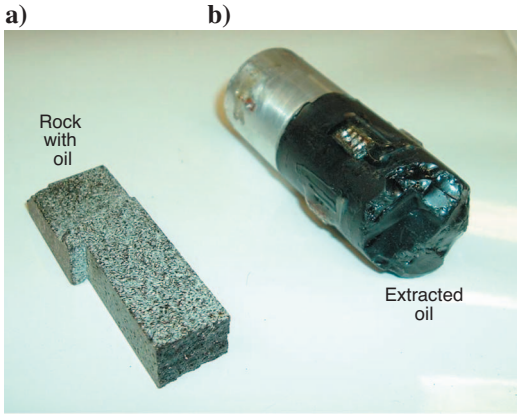

Figure 2. (a) The original Uvalde heavy-oil rock used in the experiment and (b) the extracted heavy oil.

To understand the shear behavior of heavy-oil rocks in the seismic frequency band, we describe torsional experiments in these rocks to decipher their shear moduli and shear attenuation under varying temperatures and frequencies. We examine both the rock containing the oil and the heavy oil extracted from the rock. To our knowledge, no such studies with simultaneous change in both temperature and frequency have been published in the geophysics community.

THE EXPERIMENT

Measurements are carried out using a shear rheometer as shown in Figure 3, and the experiment is schematically shown in Figure 4. Apart from the mechanical components shown in Figure 3, the rheometer consists of an assemblage of electronics and a computer interface to electronically control the mechanical parts and acquire data.

After selecting the geometry of the sample used in the analysis, the user selects the deformational sequence to be applied to the sample. The microprocessor translates the strain and strain rate history into motion of the servo-controlled motor based upon the geometry which is used. The sample is clamped at both ends, and in this case, measurements are conducted with the rock sample dry and under no lateral confining stress. The sample temperature history is controlled during the test using convected gas in the surrounding environmental chamber. A sinusoidal torsional strain is applied on one end (free end) of the sample, and the resulting response is measured by a transducer at the other end, which is fixed. From this response, the com-

Figure 3. The rheometer used in the study.

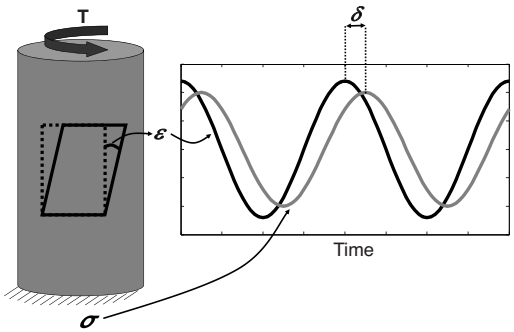

Figure 4. Schematic diagram of a harmonic loading applied to a rock sample. **T** denotes the torque applied to one end of the sample. The resulting stress (gray curve) lags behind the strain (black curve) by a phase angle δ.

puter calculates the resulting stresses and strains and generates values of the rheological properties. This method of calculating the complex shear modulus is well known in polymer science and soil science (Moyal and Fletcher, 1945; Wilhelm, 2002) and needs only minor corrections because of the geometry of the sample. In fact, this method is similar to the methodology adopted by Jackson and Paterson (1987) for rock measurements. For detailed mathematical development of the above operation, one can refer the mechanical deformation of circular and rectangular shafts found in most standard textbooks on mechanics of solids (e.g., Crandall et al., 1999).

When a viscoelastic material is subjected to a sinusoidally varying strain, a steady state will be reached where the resulting stress also is sinusoidal, with the same angular frequency, but with a phase lag of δ, which is a measure of attenuation of that body (Gray, 1972; Nowick and Berry, 1972; O'Connell and Budiansky, 1978; Chow, 1995; Braun et al., 2001; Roylance, 2001;). For an elastic material, $\delta = 0$, and for a purely viscous fluid, δ can approach $\pi/2$, whereas δ for a viscoelastic body has a value between these two limits.

The strain ϵ and stress σ can be represented by

$$\epsilon = \epsilon_0 e^{-i\omega t}, \tag{1}$$

and

$$\sigma = \sigma_0 e^{-i(\omega t-\delta)}. \tag{2}$$

The above complex form of the stress function is divided by the strain to give the complex dynamic shear modulus $\widetilde{G}$,

$$\widetilde{G} = \sigma_0'/\epsilon_0 + i\sigma_0''/\epsilon_0, \tag{3}$$

where

$$\sigma_0' = \sigma_0 \cos\,\delta, \tag{4}$$

$$\sigma_0'' = \sigma_0 \sin\,\delta. \tag{5}$$

The in-phase part of the stress σ_0' gives the real or the storage modulus G', and the out-of-phase part of the stress gives the imaginary or loss modulus G'',

$$G' = \sigma_0'/\epsilon_0, \tag{6}$$

$$G'' = \sigma_0''/\epsilon_0. \tag{7}$$

We use the common definition of the quality factor Q (inversely proportional to the attenuation coefficient) defined as (Gray, 1972; Nowick and Berry, 1972; Chow, 1995; Lakes, 1998; Braun et al., 2001; Aki and Richards, 2002;)

$$Q \equiv \frac{1}{\tan\,\delta} = 2\pi\frac{W_{st}}{W_{dis}}, \tag{8}$$

where W_{st} is the maximum elastic stored energy during a cycle of loading at the frequency under consideration and W_{dis} is the energy dissipated per cycle.

The mechanical work done over a time T is given by

$$W_{dis} = \int_T \sigma d\epsilon, \tag{9}$$

where σ is the stress and ϵ the strain. Using equation 9, W_{dis} can be calculated by integrating the out-of-phase component of stress over an entire cycle (Gray, 1972; Nowick and Berry, 1972; Chow, 1995; Braun et al., 2001; Roylance, 2001;):

$$W_{dis} = \int_0^{2\pi/\omega} (\sigma_0'' \sin\,\omega t)(-\,\epsilon_0\omega \sin\,\omega t)dt, \tag{10}$$

$$= -\,\pi\sigma_0''\epsilon_0, \tag{11}$$

$$= -\,\pi G''\epsilon_0^2. \tag{12}$$

Equation 12 can be interpreted to imply that the energy supplied to the material by the out-of-phase components is irreversibly converted to heat. Similarly, integration of the in-phase components over the full cycle yields zero work, implying that energy associated with the in-phase components is reversible, so there is no loss of energy for the in-phase components for a full cycle. The maximum energy stored by the in-phase components occurs at a quarter of the cycle and is calculated as (Gray, 1972; Nowick and Berry, 1972; Chow, 1995; Braun et al., 2001; Roylance, 2001;)

$$W_{st} = \int_0^{\pi/2\omega} (\sigma_0' \cos\,\omega t)(-\,\epsilon_0\omega \sin\,\omega t)dt, \tag{13}$$

$$= -\,\frac{1}{2}\sigma_0'\epsilon_0, \tag{14}$$

$$= -\,\frac{1}{2}G'\epsilon_0^2. \tag{15}$$

The quality factor now can be calculated from equations 8, 12, and 15:

$$Q = \frac{1}{\tan\,\delta} = \frac{G'}{G''}. \tag{16}$$

As mentioned, we use this definition (equation 16) of Q in our analysis, which also is the standard definition of Q used in physics, classical mechanics, engineering, and material science. The above definition of Q is valid for arbitrary attenuation; it is infinite for purely elastic materials and zero for completely attenuative materials.

For torsion rectangular tests, the shear modulus is given by (e.g., Zhang et al., 2003)

$$|\widetilde{G}| = \frac{ML}{BT^3\theta}\left(\frac{3 + 1.8(T/B)}{1 - 0.378(T/B)^2}\right), \tag{17}$$

where M is the torque in the torque transducer; θ is the shear angle of the motor; and L, B, and T denote the length, breadth, and thickness, respectively, of the rectangular sample. For the rheometer used in this study, the maximum error in the measured torque is 3.89

$\times 10^{-2}$ Nm, in θ is 5×10^{-5} rad, and in-phase angle δ is 1×10^{-5} rad.

We will describe the observations from the examination of heavy-oil rock and then move on to the results of analyzing the oil extracted from it.

UVALDE HEAVY-OIL ROCK

A photograph of the rock sample from Uvalde, Texas, is shown in Figure 2. This carbonate has a porosity of ≈25% and permeability of 550 mD. The typical dimensions of samples used in the study are 45 $\times$ 12.8 $\times$ 3.2 mm.

The rock is examined at temperatures ranging from 30°C to 350°C in increments of 10°C. To understand the dispersion behavior, for each temperature, the sample is analyzed for frequencies ranging from 0.01 to 80 Hz (with increments of 0.1 on the $\log_{10}$ scale). All measurements are made in the linear viscoelastic regime, which is tested by conducting a strain-sweep experiment. In a strain-sweep experiment, the modulus of the rock is measured for increasing strain amplitudes. Within the linear viscoelastic regime, the modulus does not change; and a strain amplitude lying within this linear region is selected for conducting all other temperature-frequency measurements of the rock. For testing heavy-oil rocks and the extracted oil, we use strains between 6×10^{-5} to 8×10^{-5}. Note that this strain amplitude is larger than the strains encountered in exploration seismology, where the strains are around 10^{-6} (Winkler et al., 1979). As pointed out by Iwasaki et al. (1978), higher strain amplitudes might result in lower moduli. To verify the validity of this statement, further experiments should be carried out at lower strain amplitudes using more sensitive equipment. We should, however, remember that this strain limit for linear behavior varies from one rock to another. For the time being, we assume that the higher strain does not significantly change the modulus and the relaxation mechanisms remain the same.

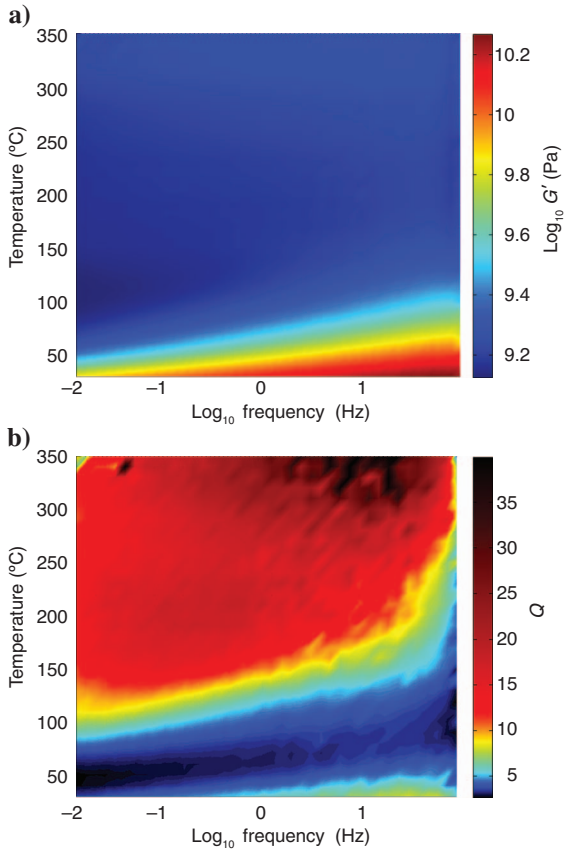

Figure 5. The shear (a) storage modulus G' and (b) quality factor Q of Uvalde heavy-oil rock. Measurements are done at temperature increments of 10°C and frequency increments of 0.1 on the $\log_{10}$ scale.

Observations

The storage modulus G' and the quality factor Q are shown in Figure 5a and b, respectively. These data have not been smoothed and are presented as collected without any processing (also, none of the data shown later have been smoothed). The maximum error in the shear modulus measurements can be found using equation 17. For example, the storage modulus at 30°C and 80 Hz is 16.97 ± 2.09 GPa and at 150°C and 0.01 Hz is 1.44 ± 0.27 GPa.

G' increases with frequency for temperatures less than ≈150°C. At higher temperatures, however, the storage modulus has a weak dependence on frequency. The strong temperature dependence of G' can be clearly seen in Figure 5a. G' is highest (≈10 GPa) at room temperature, rapidly decreases with increasing temperature, attaining a minimum value at around 150°C (this temperature-minimum changes with frequency). With further rise in temperature, G' gradually increases to approximately 1.8 GPa at 350°C. Later, we will show how well these results match with shear-wave velocities measured in the field.

Note the dependence of attenuation (inversely related to Q) on frequency (Figure 5b). A relaxation mode can be seen at temperatures less than 100°C. This relaxation is characterized by an attenuation peak or a Q trough. For example, at 70°C, the attenuation increases with increasing frequency, attains a peak at 1 Hz, then drops with further increase in frequency. The position of the relaxation peak shifts towards higher frequencies with increasing temperature.

The same attenuation peak can be better seen when plotted as a function of temperature for a particular frequency, as shown in Figure 6. Note that Q changes significantly with temperature. Q is roughly eight at room temperature (green arrow) within the seismic band and decreases with increasing temperature, attaining a value as low as four (black arrow). With yet further increase in temperature, Q increases, reaching ≈40 (purple arrow) at 350°C (Figure 6). Q at approximately 150°C (common steam-flooding conditions) for a frequency of 80 Hz is ≈5 (Figure 5b). This value is close to that observed by Macrides and Kanasewich (1987) in the steam-invaded oil

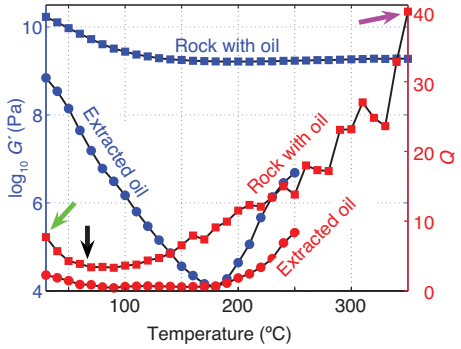

Figure 6. G' (blue curves) and Q (red curves) of Uvalde heavy-oil rock (squares) and the extracted heavy oil (circles) measured at 12.6 Hz.

sands of Clearwater Formation in Alberta, Canada. Using the spectral ratio method in a crosshole seismic experiment (90-Hz dominant frequency), they estimate the shear-wave quality factor in the steam-invaded zone to be ≈10. Though qualitatively our laboratory measurements are consistent with their field measurement (extremely low Q in both cases), there is a quantitative difference between the two quality factors, maybe arising from the fact that our experiment does not exactly simulate the in situ conditions, in addition to the heavy-oil rocks being different.

EXTRACTED HEAVY OIL

To understand the effect of the oil-phase by itself, we extract the oil from the rock by circulating solvent through it. This process of oil extraction, however, might alter the oil, and its implications are discussed later in the paper. The composition of the extracted sample is 3.5% saturates, 16.9% aromatics, 37.1% resins, and 42.5% asphaltenes. We examined the heavy oil under temperatures ranging from 30°C to 250°C at increments of 10°C, for the same frequency range as studied for the rock (0.01 to 80 Hz). All measurements are conducted in the linear viscoelastic regime under strains between 6×10^{-5} to 8×10^{-5}. The heavy oil moduli and quality factor are shown in Figure 7a and b. The heavy oil was measured under two different experimental arrangements — rectangular samples for low temperatures and thin-plate cylindrical samples for higher temperatures. This is necessary because at temperatures above ≈80°C, the rectangular samples melt and lose their shape. Therefore, thin-plate cylindrical samples are clamped between two parallel plates. At these high temperatures, some part of the oil volatilizes and might be trapped within the sample between the parallel plates. Trapping of these gaseous phases is undesirable, because it would give properties of the oil. To counter this problem, we allowed enough time for the liquefied oil sample to degassify before measurement.

Observations

The trends observed for the mechanical properties of the rock resemble those for the extracted oil. This supports the conclusion that the behavior of the heavy oil within the rock dominates the mechanical response of the rock with changing temperature and frequency. This is expected because with changing temperature and frequency there would be a significantly greater change in the physical and chemical properties of the oil compared with that of the rock matrix. The oil shows noticeable dispersion for temperatures less than ≈180°C (Figure 7a). At higher temperatures, however, the storage modulus is nearly constant with frequency. With increasing frequency, G' generally increases for all temperatures.

The strong temperature dependence of G' can be clearly seen from Figure 7a. G' is highest (≈1.0 GPa) at room temperature in the seismic band and decreases rapidly with increasing temperature, attaining a minimum value at around ≈180°C (as for the rock, the value of this minimum and the temperature of its occurrence changes with frequency). With further rise in temperature, G' increases to about 0.002 GPa at 250°C.

The quality factor Q (Figure 7b) shows a moderately weak dependence on frequency, with some general increases of Q with frequency. There seems to be a relaxation mechanism active in the temperature range of 50°C to 100°C, where Q initially decreases with frequency, reaches a trough, and then subsequently increases with further increase in frequency. The minimum Q in this region is close to zero. The position of this minimum shifts to higher frequencies with increasing temperature.

Not surprisingly, Q changes significantly with temperature. The quality factor of the oil is ≈2.5 at room temperature in the seismic band, and decreases with increase in temperature, attaining a value close to zero as the oil goes through the relaxation mechanism. With yet further increase in temperature, Q initially increases and then drops before increasing again. This can be clearly seen at 0.01 Hz, where Q increases after the initial relaxation trough at 60 °C (Figure 7b). At higher temperatures, melting of the oil reduces Q, and it attains values as low as 0.2 at 140°C. With further heating, Q rises again instead of dropping. This is surprising because with increasing temperature, the oil should approach a Newtonian fluid and its shear modulus should approach zero instead of rising.

MECHANISMS

The strong temperature dependence of the modulus and the attenuation correspond to the melting of the heavy oil and its subsequent composition change at high temperatures. Nur et al. (1984) suggest that this change in the heavy oil would translate to a significant change in the mechanical response of the rock containing the heavy oil.

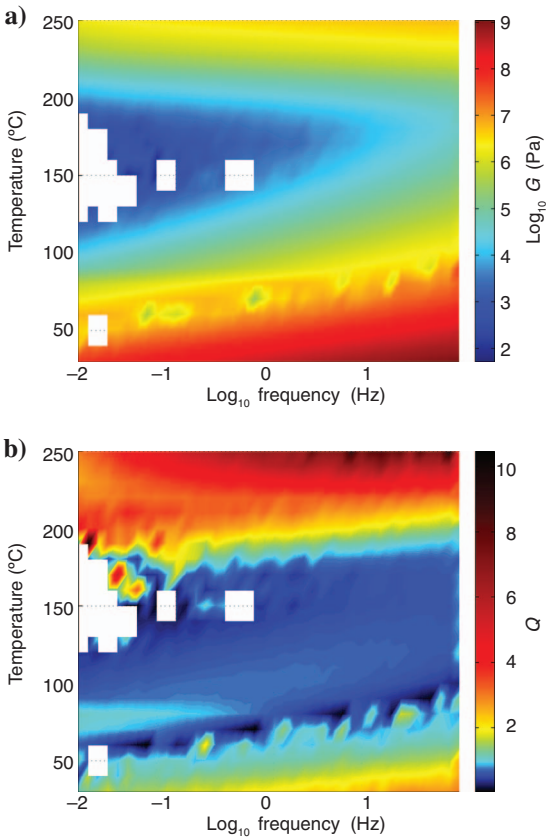

Figure 7. The shear (a) storage modulus G' and the (b) quality factor Q of the oil extracted from the Uvalde heavy-oil rock. Measurements are done at temperature increments of 10°C and frequency increments of 0.1 on the $\log_{10}$ scale. The missing data points correspond to erroneous results (e.g., negative moduli) arising from noise and/or experimental errors and/or for measurements lying outside the sensitivity limit of the rheometer.

The increase in G' of the rock with frequency is consistent with the frequency dependence of G' of the extracted heavy oil. Heavy oil is viscoelastic, so at low frequencies the molecules/chains in the viscoelastic material have time to come to equilibrium, resulting in a low storage modulus. In contrast, at relatively higher frequencies the molecules/chains do not have sufficient time to relax as they are tangled and locked, thereby making the material stiffer (high G'), as there is a more efficient transfer of mechanical energy between the molecules/chains. Also, at low frequencies the material has sufficient time to relax almost completely as the molecules/chains slide past each other, which minimizes the energy loss (high Q). The locking of the molecules/chains at higher frequencies translates to a high value of Q, as relative sliding is inhibited, lowering frictional loss.

For intermediate frequencies, however, the molecules/chains have a maximum slip during a cycle of loading, leading to maximum frictional loss of energy. This is similar to maximum dielectric losses occurring at molecular resonant frequencies (Strobl, 1997). Here, an analogy can be drawn with the Maxwell model comprising of a spring and a dashpot in series. At high frequencies, the dashpot has little time to move and thus the system responds elastically (high Q). At intermediate relaxation frequencies, the frequency of vibration matches the rate of movement of the piston in the dashpot, resulting in a maximum loss of energy (low Q). When the system is vibrated at a low frequency, the piston moves by the same amount as for the resonant frequencies. However, because the time period of each cycle is now long, most of the cycle is dominated by elastic movement of the spring (after the piston in the dashpot has seen its maximum displacement). This results in a relatively large storage energy compared with the energy dissipated (high Q).

The high frictional loss of energy in the rock manifests in a relaxation trough or attenuation peak (Ferry, 1980) seen in Figure 5b. We believe this attenuation peak is caused by viscous relaxation of the heavy oil within the rock (Walsh, 1968, 1969). As described by O'Connell and Budiansky (1977), this relaxation occurs between the saturated isolated (at low frequencies, the shear stresses in the fluid relax completely, but no fluid flows out of the pores/cracks) and glued cases (at high frequencies, the viscosity of the fluid is high and the shear stresses in the fluid do not relax).

If Coulomb frictional sliding between crack surfaces and grain boundary contacts is assumed to be the dominant attenuation mechanism, Q should be independent of frequency (Johnston and Toksöz, 1981). Hence, the frequency dependence of Q rules out friction as the dominant attenuation mechanism.

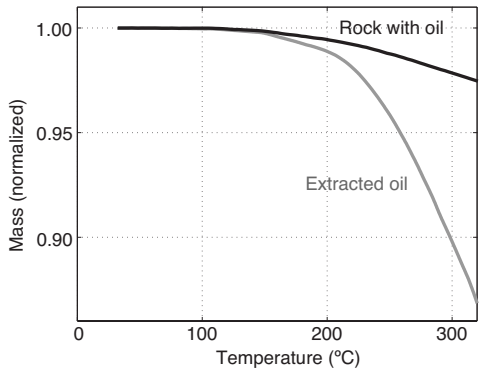

Figure 8. Thermogravimetric analysis (TGA) of Uvalde heavy-oil rock (black line) and the oil extracted from it (gray line).

One might speculate that squirt flow (Mavko and Nur, 1975; O'Connell and Budiansky, 1977; Vo-Thanh, 1990) also could result in such a relaxation peak. The high viscosity of heavy oil at these low temperatures, however, makes squirting of these oils unlikely. This is supported by the modeling done by Wolf et al. (2006). One way of helping to understand these observations would be to model the response and compute the aspect ratio of the cracks, as suggested and implemented by O'Connell and Budiansky (1977) and Vo-Thanh (1990).

Another way of identifying possible mechanisms is to analyze the dynamic mechanical response of the heavy oil extracted from the rock. If indeed viscous relaxation is taking place, we should also observe a relaxation peak in the heavy oil at the same temperatures and frequencies as those in the heavy-oil rock; otherwise, some mechanism such as squirt flow might be taking place. The two relaxations in Figures 5b and 7b are taking place at identical temperatures and frequencies, thereby strongly implying that viscous relaxation of the heavy oil within the rock is responsible for the observed attenuation peak. The shift in the attenuation peak toward lower frequencies with decreasing temperature occurs because the effect of decreasing frequency (longer flow time) counteracts the effect of the decreasing temperature (increased viscosity) so as to sustain the viscous relaxation of the oil.

As mentioned earlier, the strong temperature dependence of the mechanical properties of the heavy-oil rock comes from the reduced viscosity or melting of the heavy oil (glass transition temperature of $\approx$30°C of the heavy oil) and its subsequent composition change at high temperatures. Low values of Q, approaching zero (around 70°C), at this relaxation are the result of the relative movement of the molecular constituents of the heavy oil. Note that the low Q values near 150°C are a result of the more fluid-like behavior of heavy oil, i.e., it behaves as a Newtonian fluid at these temperatures. This low-temperature window would correspond to common steamflooding conditions.

The rise in G' and Q for temperatures exceeding 150°C is probably caused by a compositional change in the heavy oil, wherein the lighter components are lost, leaving the heavier asphaltenes behind (Lesueur and Gerard, 1996; Deshpande et al., 2003). Asphaltenes are essentially solid particles (Lesueur and Gerard, 1996) that increase the modulus and Q of the oil. If the experiment is now repeated with this modified oil, we expect to observe hysteresis.

This compositional change can be corroborated from thermogravimetric analysis (TGA), which in Figure 8 shows the mass of the heavy oil decreasing with increasing temperature. A significant drop in mass at $\approx$150°C corresponds to the loss of the lighter components, thereby making the heavy oil stiffer and less attenuative. One issue that has been raised is possible liberation of CO_2 from the carbonate minerals above 110°C. This is not possible for extracted oils because no carbonate is present. No loss of mass is detected in the TGA results for the cleaned carbonate matrix under our temperature conditions.

An alternative cause for the increase in G' and Q would be polymerization of the oil. At high temperatures, and in hydrogen-poor environments, hydrocarbons can cross-link and form complex polymer networks typical of plastics. The temperatures in our experiment, however, are considered too low to induce significant bond cleavage and initiate polymerization (Hunt, 1996).

The G' for the oil, however, is lower than the rock moduli (Figure 6) because the solid grains making up the rock matrix are stiffer than the oil. The change in G' with temperature for the rock is smaller than that for the oil because the solid rock frame supports shear at all temperatures. The high G' of the rock relative to that of the oil (difference of a few orders in magnitude) at these high temperatures (greater than 150°C) makes the contribution of the oil modulus negligible at high temperatures. At these high temperatures, the negligible dispersion suggests that friction might be a dominant attenuation mechanism. However, other mechanisms, such as squirt flow and viscous losses in the oil, cannot be completely ruled out.

MODELING

In practice, velocity measurements do not exist for all temperatures and frequencies. This necessitates the use of modeling to provide the missing data. Laboratory data can be used to establish the right model. Modeling also has another advantage: It can help in uncertainty analysis.

After extensive analysis, we found that the Cole-Cole model (Cole and Cole, 1941) provides a good fit to the observed data unlike Wolf et al. (2006) who suggest using the simpler Maxwell model. This should be expected because the relaxation peak for heavy oils is broad because of their complex composition and so cannot be described by using a Maxwell model. According to the Cole-Cole model, the dynamic complex shear modulus $\widetilde{G}(\omega)$ is given by,

$$\widetilde{G}(\omega) = G_\infty - \frac{G_\infty - G_0}{1 + (i\omega/\omega_r)^\alpha}, \tag{18}$$

where G_0 and G_∞ are the shear moduli at zero and infinity frequencies, respectively. The parameter ω_r is the relaxation frequency or the frequency at which the attenuation peak is observed and is given by

$$\omega_r = \frac{G_\infty - G_0}{\eta}, \tag{19}$$

where η is the viscosity. As observed by Gautam et al. (2003), the complex composition of heavy oils might result in smearing of the relaxation peak, which is controlled by the parameter α.

The result from Cole-Cole modeling of heavy-oil rock at 70°C is shown in Figure 9a along with their 95% confidence intervals. The procedure for computation of the confidence intervals is provided in Appendix A. Note the good match between the data and the model. Usually, the modeling parameters are all assumed to be real numbers, but our analysis shows that if these parameters are allowed to be complex, the fit is better, as seen in Figure 9b. Complex G_0, G_∞, and η imply that all the elements in the Cole-Cole model are viscoelastic. For an isolated relaxation mechanism, real model parameters ought to be used in equation 18. In reality, however, there might be overlap among different relaxations present at various frequency ranges. Under these circumstances, using complex model parameters in the Cole-Cole model (equation 18) would yield a better fit.

Modeling also helps in comparing the velocity data collected in the laboratory with the velocity observed in the field. Shear-wave velocities were computed from the P-wave velocities given in Schmitt (1999) by assuming a constant (with frequency) Poisson's ratio of 0.16. The two velocities, one computed from a VSP measurement (100 Hz) and the other a sonic log measurement (10 KHz), are shown in Figure 9a and b. There is a good match between our laboratory measurements and transformed field velocities, implying that the Cole-Cole model potentially can be used to predict data. This emphasizes that our laboratory measurements potentially can be directly applicable in seismic data analysis.

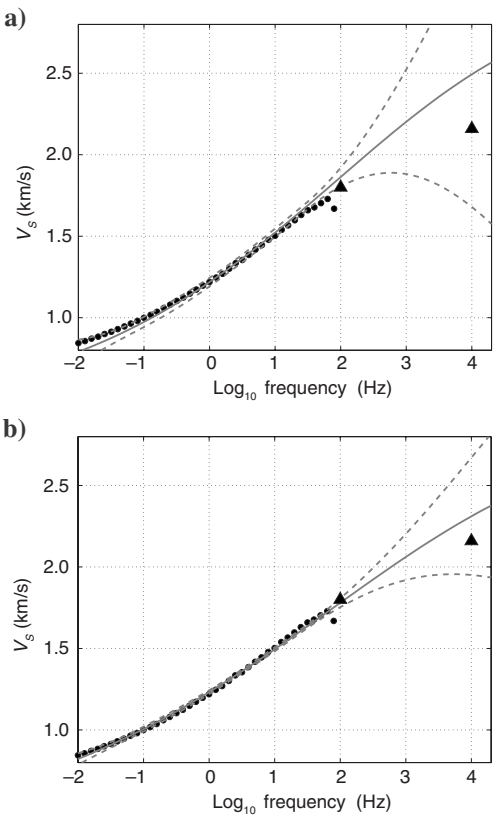

Figure 9. The laboratory-measured (black dots) shear velocity (V_S) of the Uvalde heavy-oil rock at 70 °C with the Cole-Cole fit (solid gray curve) and 95% confidence intervals (dashed gray curves) with (a) real model parameters and (b) complex parameters. Two shear velocities estimated from Schmitt (1999) are marked by ▲. The model parameters used in (a) are $G_0 = 0.48$ GPa, $G_\infty = 21.48$ GPa, $\eta = 0.0035$ GPa/s, and $\alpha = 0.261$, and in (b) are $G_0 = 0.3 - i0.05$ GPa, $G_\infty = 19.37 + i0.87$ GPa, $\eta = 0.0026 + i0.0004$ GPa/s, and $\alpha = 0.225 + i0.0026$.

CONCLUSIONS

Unlike common fluids (e.g., brine and light oil), heavy oils found in heavy-oil rocks act as solids at room temperature and fluids at higher temperatures. In other words, at room temperature, heavy oils support a shear wave, but not at higher temperatures where the shear modulus approaches zero. They would, however, have a nonzero bulk modulus at all temperatures, and the percentage change in the bulk modulus would be smaller compared with the change in shear properties. Thus, shear information is more attractive and can be more diagnostic than bulk modulus properties and so makes acquisition of multicomponent seismic data all the more important.

Our shear-wave measurements, as a function of temperature, represent conditions encountered during in situ steam flooding of heavy oil reservoirs. Moreover, as heavy-oil rocks are effectively viscoelastic, their properties in the seismic band would differ significantly from that in the logging-frequency range and the ultrasonic

band. The shear properties, acquired at frequencies ranging from 0.01 to 80 Hz (which includes the seismic band), should be close to the seismic properties of heavy oils in the field.

The significant frequency dependence of the moduli and attenuation within the seismic bandwidth for heavy oils, makes exploitation of frequency-dependent properties promising. Moreover, there would be significant differences in properties among seismic, log, and ultrasonic frequencies for heavy-oil rocks. Most of the existing methods for Q estimation from field data assume a constant Q within the seismic bandwidth, a poor approximation as shown by our laboratory measurements.

The strong temperature dependence of the mechanical properties of heavy oils makes 4D-9C seismic analysis promising. Temperature has a dramatic influence on velocity, as well as on attenuation, and thus on traveltimes and amplitudes of shear waves. For example, on heating a heavy oil reservoir, the shear-wave velocity might decrease by a factor of three, whereas the quality factor can decrease by a factor of 10. Seismic data can be exploited to estimate the physical state of the rock and thus the local temperature. As seen in many studies, the direction and extent of the steam front can be detected from seismic data. An important application for shear data would be to monitor the temperature or formation of a collapse zone within the oil sand reservoir to distinguish this from the steam-invaded zone (change in fluid phase) using the V_P-V_S ratio.

ACKNOWLEDGMENTS

We appreciate Ken Larner's help in editing this manuscript, and also the help of Luis Tenorio on statistical analysis of the data. The support for this work was provided by the sponsors of Center for Wave Phenomena and Center for Rock Abuse. We value Merrick Johnston's help in collecting part of the TGA data. We also would like to thank Xiaoxia Xu, Manika Prasad, and Rodrigo Fuck for many fruitful discussions. The suggestions and comments from Kees Wapenaar, Yonghe Sun, Konstantin Osypov, and two other anonymous reviewers helped improve the manuscript.

APPENDIX A

CONFIDENCE INTERVALS FOR THE COLE-COLE NONLINEAR MODEL

One way of determining the validity of a model (Cole-Cole model in our case) fit to the observed data is to construct confidence intervals. We follow the procedure described by Rawlings et al. (1998) to construct confidence intervals for fitting models with nonlinear parameters.

For a normal distribution of errors ϵ (difference between the model and observations), Gallant (1987) shows that

$$\hat{\theta} \dot{\sim} N[\theta, (\mathbf{F}'\mathbf{F})^{-1}\sigma^2], \tag{A-1}$$

where θ is the vector of p ($p = 4$ for Cole-Cole model) model parameters, $\hat{\theta}$ is the least-squares estimate of θ, the symbol $\dot{\sim}$ denotes approximately distributed, N denotes normal distribution, $\mathbf{F}$ is the $n \times p$ matrix of partial derivatives (n being the number of data points), and σ is the standard deviation in errors ϵ. $\mathbf{F}(\theta)$ can be computed as $\mathbf{F}(\hat{\theta})$, and σ can be estimated from $s^2(\hat{\theta}) = SS[\mathrm{Res}(\hat{\theta})]/(n - p)$ ($SS[\mathrm{Res}(\hat{\theta})]$ being the sum of the squares of the residuals), which gives the estimated variance-covariance matrix for $\hat{\theta}$ as

$$\mathbf{s}^2(\hat{\theta}) = (\mathbf{F}'\mathbf{F})^{-1}\mathbf{s}^2. \tag{A-2}$$

For the Cole-Cole model (equation 18), the partial derivatives are

$$\frac{\partial \tilde{G}(\omega)}{\partial G_\infty} = 1 - \frac{1}{1 + (i\omega/\omega_r)^\alpha}, \tag{A-3}$$

$$\frac{\partial \tilde{G}(\omega)}{\partial G_0} = \frac{1}{1 + (i\omega/\omega_r)^\alpha}, \tag{A-4}$$

$$\frac{\partial \tilde{G}(\omega)}{\partial \omega_r} = \frac{(G_\infty - G_0) i\omega \left(\frac{i\omega}{\omega_r}\right)^{(-1+\alpha)} \alpha}{(1 + (i\omega/\omega_r)^\alpha)^2 \omega_r^2}, \tag{A-5}$$

$$\frac{\partial \tilde{G}(\omega)}{\partial \alpha} = \frac{(G_\infty - G_0)\left(\frac{i\omega}{\omega_r}\right)^\alpha Log\left[\frac{i\omega}{\omega_r}\right]}{(1 + (i\omega/\omega_r)^\alpha)^2}. \tag{A-6}$$

Confidence intervals for any other nonlinear function $h(\theta)$ can be calculated from $h(\hat{\theta})$, which is approximately normally distributed with mean $h(\theta)$ and variance $\mathbf{H}(\mathbf{F}'\mathbf{F})^{-1}\mathbf{H}'\sigma^2$ (Gallant, 1987), where $\mathbf{H}$ is the partial derivative matrix of $h(\theta)$ with respect to the p model parameters. The variance of $h(\hat{\theta})$ can be estimated by

$$\mathbf{s}^2[\mathbf{h}(\hat{\theta})] = [\hat{\mathbf{H}}(\hat{\mathbf{F}}'\hat{\mathbf{F}})^{-1}\hat{\mathbf{H}}']\mathbf{s}^2. \tag{A-7}$$

The approximate $100(1 - \alpha)\%$ confidence interval estimate of $h(\theta)$ is given as

$$h(\hat{\theta}) \pm t_{[\alpha/2,(n-p)]}[\hat{\mathbf{H}}(\hat{\mathbf{F}}'\hat{\mathbf{F}})^{-1}\hat{\mathbf{H}}'\mathbf{s}^2]^{1/2}, \tag{A-8}$$

where t is the Student's t distribution. If the functions of interest are the n values of $\hat{Y}_i$ (the measured values), then $\mathbf{H}(\hat{\theta}) = \mathbf{F}(\hat{\theta})$ (Rawlings et al., 1998). For functions of interest other than the n values of $\hat{Y}_i$ (seen in Figure 9a and b, for instance), we need to compute $\mathbf{H}(\hat{\theta})$ for the additional functions of interest.

REFERENCES

Aki, K., and P. G. Richards, 2002, Quantitative seismology, 2nd ed.: University Science Books.

Batzle, M., R. Hofmann, and D. Han, 2006, Heavy oils — Seismic properties: The Leading Edge, **25**, 750–756.

Batzle, M., R. Hofmann, M. Prasad, G. Kumar, L. Duranti, and D. Han, 2005, Seismic attenuation: Observations and mechanisms: 75th Annual International Meeting, SEG, Expanded Abstracts, 1565–1569.

Braun, S., D. Ewins, and S. S. Rao, 2001, Encyclopedia of vibration: Academic Press Inc.

Cole, K. S., and R. H. Cole, 1941, Dispersion and absorption in dielectrics — I, alternating current characteristics: Journal of Chemical Physics, **9**, 341–351.

Chow, T. L., 1995, Classical Mechanics: John Wiley & Sons.

Crandall, S. H., N. C. Dahl, and T. J. Lardner, 1999, An introduction to the mechanics of solids: Second edition with SI units: McGraw-Hill Book Co.

Curtis, C., R. Kopper, E. Decoster, A. G. Garcia, C. Huggins, L. Knauer, M. Minner, N. Kupsch, L. M. Linares, H. Rough, and M. Waite, 2002, Heavy-oil reservoirs: Oilfield Review, **14**, 30–51.

Deshpande, A. P., S. Varughese, A. Shahanawaz, and M. V. Arun, 2003, Microstructure-related rheological behavior of asphalt: IIT-Madras, Chennai.

Ferry, J. D., 1980, Viscoelastic properties of polymers: John Wiley & Sons.

Gallant, A. R., 1987, Nonlinear statistical models: John Wiley & Sons.

Gautam, K., M. Batzle, and R. Hofmann, 2003, Effects of fluids on attenuation of elastic waves: 73rd Annual International Meeting, SEG, Expanded Abstracts, 1592–1595.
Gray, D. E., 1972, American Institute of Physics handbook, 3rd ed.: McGraw-Hill Book Co.
Han, D., J. Liu, and M. Batzle, 2005, Measurement of shear wave velocity of heavy oil: 75th Annual International Meeting, SEG, Expanded Abstracts, 1513–1517.
Hedlin, K., L. Mewhort, and G. Margrave, 2001, Delineation of steam flood using seismic attenuation: 71st Annual International Meeting, SEG, Expanded Abstracts, 1572–1575.
Hunt, J. M., 1996, Petroleum geochemistry and geology: W. H. Freeman & Co.
Iwasaki, T., F. Tatsuoka, and Y. Takagi, 1978, Shear moduli of sand under cyclic torsional shear loading: Soils and Foundations, **18**, 39–56.
Jackson, I., and M. S. Paterson, 1987, Shear modulus and internal friction of calcite rocks at seismic frequencies: Pressure, frequency, and grainsize dependence: Physics of Earth and Planetary Interiors, **45**, 349–367.
Jenkins, S. D., M. W. Waite, and M. F. Bee, 1997, Time-lapse monitoring of the Duri Steam-flood, A pilot and study case: The Leading Edge, **16**, 1267–1273.
Johnston, D. H., and M. N. Toksöz, 1981, Definitions and terminology, *in* M. N. Toksöz and D. H. Johnston, eds., Seismic wave attenuation: SEG.
Lakes, R. S., 1998, Viscoelastic solids: CRC Press.
Lesueur, D., and J. F. Gerard, 1996, A structure-related model to describe asphalt linear viscoelasticity: Journal of Rheology, **40**, 813–836.
Macrides, C. G., and E. R. Kanasewich, 1987, Seismic attenuation and Poisson's ratios in oil sands from crosshole measurements: Journal of the Canadian Society of Exploration Geophysicists, **23**, 46–55.
Mavko, G., and A. Nur, 1975, Melt squirt in the asthenosphere: Journal of Geophysical Research, **80**, 1444–1448.
Moyal, J. E., and W. P. Fletcher, 1945, Free and forced vibration methods in the measurement of the dynamic properties of rubbers: Journal of Scientific Instruments, **22**, 167–170.
Nowick, A. S., and B. S. Berry, 1972, Anelastic relaxation in crystalline solids: Academic Press Inc.
Nur, A., C. Tosaya, and D. Vo-Thanh, 1984, Seismic monitoring of thermal enhanced oil recovery processes: 54th Annual International Meeting, SEG, Expanded Abstracts, 337–340.
O'Connell, R. J., and B. Budiansky, 1977, Viscoelastic properties of fluid-saturated cracked solids: Journal of Geophysical Research, **82**, 5719–5735.
———, 1978, Measures of dissipation in viscoelastic media: Geophysical Research Letters, **5**, 5–8.
Rawlings, J. O., S. G. Pantula, and D. A. Dickey, 1998, Applied regression analysis — A research tool: Springer texts in statistics, 2nd ed.: Springer-Verlag.
Roylance, D., 2001, Engineering viscoelasticity: Course notes, Massachusetts Institute of Technology.
Schmitt, D. R., 1999, Seismic attributes for monitoring of a shallow heated heavy oil reservoir: A case study: Geophysics, **64**, 368–377.
Strobl, G., 1997, The physics of polymers — Concepts for understanding their structures and behaviors: Springer-Verlag.
Vo-Thanh, D., 1990, Effects of fluid viscosity on shear-wave attenuation in saturated sandstones: Geophysics, **55**, 712–722.
Walsh, J. B., 1968, Attenuation in partially melted material: Journal of Geophysical Research, **73**, 2209–2216.
———, 1969, New analysis of attenuation in partially melted material: Journal of Geophysical Research, **74**, 4333–4337.
Watson, I. A., K. F. Brittle, and L. R. Lines, 2001, Heavy-oil reservoir characterization using elastic wave properties: CREWES Research Report, 13, 777–784.
Wilhelm, M., 2002, Fourier-transform rheology: Macromolecular Materials and Engineering, **287**, 83–105.
Winkler, K., A. Nur, and M. Gladwin, 1979, Friction and seismic attenuation in rocks: Nature, **277**, 528–531.
Wolf, K., T. Mukerji, and G. Mavko, 2006, Attenuation and velocity dispersion modeling of bitumen saturated sand: 76th Annual International Meeting, SEG, Expanded Abstracts, 1993–1997.
Zhang, Y., D. Rodrigue, and A. Aït-Kadi, 2003, Torsion properties of high density polyethylene foams: Journal of Cellular Plastics, **39**, 451–474.